

Comparative Structural Characterization of Fiber Reinforced Composite Rotating Disc: A Validated Investigation

G.R. Kumar^a, R. Vijayanandh^{b,*}, M.B. Kamaludeen^c, S. Balasubramanian^d, P. Jagadeeshwaran^e, M. Ramesh^f

^{a, b} Assistant Professor, ^f UG Student, Department of Aeronautical Engineering, ^d Associate Professor, Department of Mechanical Engineering, Kumaraguru College of Technology, Coimbatore, Tamil Nadu, India,

^c Department of Mechanical Engineering, Crescent Institute of Science and Technology, Chennai, Tamil Nadu, India,

^e Rajalakshmi Institute of Technology, Chennai, Tamil Nadu, India.

Keywords:

Composite Materials
Ceramics
FEA
Rotating Disc
Structural analysis

ABSTRACT

The objective is to determine the mechanical behavior of fiber-reinforced composite of a rotating disc by using experimental and Finite Element Analysis (FEA) studies. Firstly, the FEA analysis have been conducted for two different families under the loading conditions of 600 RPM as rotational velocity with external frictional force as 10 N. In which, the seven different composite specimens such as Epoxy-Carbon-UD-Prepreg-SiC, Epoxy-Carbon-UD-Wet-SiC, Epoxy-Carbon-Woven-Prepreg-SiC, Epoxy-Carbon-Woven-Wet-SiC, Epoxy E-Glass-UD-SiC, Epoxy-E-Glass-Wet-SiC and Epoxy-S-Glass-UD-SiC are undergoing for structural characterization analysis with help of FEA tool. Apart from these materials, the four base materials were also analyzed through FEA for comparison under the same loading conditions. Secondly, the experimental study was conducted to investigate the applicability of the FRP solid disc brake rotor with Silicon Carbide (SiC), in this regard the ASTM standard specimens based pin on disc apparatus for Carbon Woven based Ceramic-composite was prepared. The validation is also executed in between displacements of these two approaches. Finally, this work confirmed that the carbon fiber ceramic matrix composite materials are the good materials to resist rotodynamic loads therefore the work also strongly recommended that CCMC to be implemented in the fabrication of rotating components like aircraft and automotive disc brakes.

* Corresponding author:

R. Vijayanandh 
E-mail: vijayanandh.raja@gmail.com

Received: 31 May 2020

Revised: 16 August 2020

Accepted: 4 October 2020

© 2020 Published by Faculty of Engineering

1. INTRODUCTION

This study aims to investigate the strength of different composite specimens using pin on disc

experiment and FEA analysis through the estimations of deformations, stress distributions, and frictional forces under rotational loads. Especially, the FEA analysis is used to identify the

shear stress of various composite as well as suggest the optimized materials for the implementation in the rotating component-based applications. This work has merit to serve as a reference case to study more complex situations such as the confidence approach of FRP aircraft disk brake during mechanical testing.

The matrix composites are reinforced with continuous reinforcement, such as particles, whiskers or chopped fibers or with continuous fibers. In this paper, polymer fiber is used as reinforcement, which primarily focuses to provide toughness to the brittle matrix. Filler materials in particle form are also sometimes added to the matrix materials during the processing of CMCs (Ceramic Matrix Composites) to enhance properties such as electrical conductivity, thermal conductivity, thermal expansion, and hardness. Particles with different shapes such as spherical, irregular, and faceted are commonly used during the processing of CMCs. It has been used in civil, aerospace, and automobile applications due to advantageous properties such as high specific strength, stiffness, low weight, and corrosion resistance [1]. In aforesaid applications, various composite parts are joined or fastened together using either adhesives or metal fasteners. The ceramic disc brake is structurally more efficient than metals/Alloys because they provide better opportunities to eliminate stress concentrations [2]. In this paper primary deals the structural and tribological behaviour of Carbon Fibre Reinforced Polymer (CFRP) which is an extremely strong and light fiber-reinforced plastic that contains carbon fibers. CFRPs can be expensive to produce but are commonly used wherever high strength-to-weight ratio and rigidity are required, such as aerospace and automotive industries. The binding polymer is a thermoset resin epoxy. The properties of the final CFRP product can also be affected by the type of additives introduced to the binding matrix (the resin). To provide the following advantages in engineering applications CFRP based CMC is the best implementation: reduction in weight, reduction in the number of brakes per axle, and stable friction from very high speeds and all temperatures [3 - 4].

2. LITERATURE SURVEY

The collection of relevant useful research works can able to provide the right and good manner of

problem's solution techniques for complicated problems. In this work, the following literature is used: The article [1] analyzed the aluminium matrix composite with the addition of SiC. In which he proved that SiC has capable to resist wear and frictional behavior underpin on disc experiment. The article [2] investigated the comparative studies on various ceramic-based fillers such as SiC, aluminum oxide, and fly-ash with glass polyester composite by the support of various relevant experimental tests. In which, SiC performed well than other fillers in all the mechanical perspectives with the inclusion of glass fiber composites. The article [3] experimentally tested the shear strength behaviors on various weight percentages of SiC with advanced fibers such as Carbon, Glass, and Kevlar. From these comparative analyses, it was understood that the Glass fiber-based composites were performed well at the low content level of SiC thus glass fiber is also good rapport with SiC filler. All these works were clearly explained about the importance of the use of SiC. The article [4] conducted the comparative analyses on variational frictional studies on carbon fiber reinforced composites, which undoubtedly provided the detail about carbon fiber-based composites and its fillers in this current work [5] comprehensively analyzed the frictional manners on different carbon-based composites such as carbon particulate based composite, carbon fiber-based composites. In that, the carbon fiber bound with ceramic filler composites were performed well than other carbon composites. Thus in this work strongly confirmed that fiber-based composites were more suitable to work as material in this comparative analysis on rotating disc. The fundamental application of this work is disc brake, in which thermal failure, frictional issue, wear affect are predominantly reduce the lifetime of a rotating disc brake thus in this current study the same aforesaid factors are considered as major problems. To tackle these non-linear factors the [6] article supported a lot, in this article, the author mentioned the failure issues in the rotating disc also suggested implementing carbon fiber-based ceramic composite material in the rotating component, which provided more confident to continue this current investigation. The article [7] conducted the pin on disc-based experimental investigations on glass fiber composites with graphite filler, in which the following outcomes

were understood: glass fibers are user friendly with graphite filler, naturally glass fiber-based composites have the resistance in-build power, and graphite is a perfect filler to enhance the composite's wear property.

2.1 Summary

The type of fibers selected will depend on the application, fiber characteristics, fiber orientation, and bonding properties with respect to the functions of matrix materials [8 - 11]. The seven different composite specimens are used such as Epoxy-Carbon-UD-230GPa-Prepreg-SiC, Epoxy-Carbon-UD-230GPa-Wet-SiC, Epoxy-Carbon-Woven-23GPa-Prepreg-SiC, Epoxy-Carbon-Woven-230GPa-Wet-SiC, Epoxy-E-Glass-UD-SiC, Epoxy-E-Glass-Wet-SiC and Epoxy-S-Glass-UD-SiC for this work. Aside from the material selection, the clear views to implement and execute the methodologies used are extracted from this standard literature survey. Especially in the experimental test, the specimen preparation, suitable manufacturing technology, environmental conditions for test are captured. And then in FEA analysis, the boundary conditions, the mechanical properties of all the ingredients in composites, solver control, and its procedures are gained from the literature work.

3. METHODOLOGY

In this comparative analysis, the FEA based engineering approach is predominantly used, in which all the conclusions of this work are finalized through FEA only. In general, FEA has less in the production of reliable output, so the pin on disc based experimental tests are conducted for validation and thus this implemented FEA's reliability could increase.

3.1 Modeling and Meshing of FEA

The computational model of the brake disc is created using CATIA software and imported into FEA ANSYS for meshing conditions. The 3D layered tetrahedral element, adhesive layer are glued together using Boolean operation. Finer mesh used in the model for applying the boundary conditions to form the completed design of disc brake [12-13]. The following dimensions used for the conceptual design model as shown in Table 1. After the successful

generation of the conceptual design of the test specimen, the discretization process is executed successfully for the purpose to create the load observing behavior in the test model. The entire discretization processes are successfully executed with the help of ANSYS Mesh Tool 16.2, which is a perfect mesh tool to create 3-D discretization. The fine and un-structural mesh elements are used in this work, in which proximity and curvature facilities are used for the creation of good quality mesh. The quality of the mesh is 0.78. The complete meshing of the Carbon/SiC-based composite laminates in a more sensitive manner by dividing it into small elements as shown in Figs. 1 to 5.

Table 1. Design parameters for Disc brake model.

Design parameters	Dimensions (mm)
The outer diameter of the base	55
The thickness of the base	10
The diameter of the center hole	13
The diameter of the top tool	6
Length	10

3.2 Boundary Conditions Used in FEA

In this work, two different FEA tools are used which are ANSYS ACP 16.2 and ANSYS Structural tool 16.2. In ANSYS ACP 16.2, the controlled composite generations are executed, in which the vital tools of fiber orientation, matrix implementation, and mixture inclusion are implemented. The reliable output execution through computational simulations is achieved with the help of good boundary conditions such as support details, mechanical properties of the materials used, and implementations of needful and relevant loads [14]. In ANSYS Structural tool 16.2, the pre-processing, solving, and post-processing of the shear test based structural analyses are completed with the help of good boundary conditions. The vital boundary conditions used in this work are, Joint fixed-ground supports are given at the mid hole of the base, fixed support is given at the top face of the top tool, the amount of 10 N is given at the bottom face of the top tool and rotational velocity of 600 RPM is given at the base. The total deformation, shear stress, and equivalent stress are the primary outputs that are computed with the help of the FEA tool [15].

3.3 Mathematical Modeling used in this FEA

In general, mathematical modeling consists of governing equations defined in a field and boundary conditions provided at the boundaries of the area. In this work, the composites are primary platforms so two more important equations are needed to be included to provide required and acceptable outputs. The important equations are 3-D Hooke's law equation and strain-displacement relationships [1-10]. Finally, fifteen sub-equations are predominantly used in this FEA based frictional stress calculations, which are:

Force balance in r-direction

$$\frac{1}{r} \frac{\partial}{\partial r} (r\sigma_{rr}) + \frac{1}{r} \frac{\partial \sigma_{r\theta}}{\partial \theta} + \frac{\partial \sigma_{rz}}{\partial z} - \frac{\sigma_{\theta\theta}}{r} + \rho f_r = \rho a_r \quad (1)$$

Force balance in θ the direction

$$\frac{1}{r} \frac{\partial}{\partial r} (r\sigma_{r\theta}) + \frac{1}{r} \frac{\partial \sigma_{\theta\theta}}{\partial \theta} + \frac{\partial \sigma_{\theta z}}{\partial z} - \frac{\sigma_{r\theta}}{r} + \rho f_\theta = \rho a_\theta \quad (2)$$

Force balance in the z-direction

$$\frac{1}{r} \frac{\partial}{\partial r} (r\sigma_{rz}) + \frac{1}{r} \frac{\partial \sigma_{\theta z}}{\partial \theta} + \frac{\partial \sigma_{zz}}{\partial z} + \rho f_z = \rho a_z \quad (3)$$

Normal Strain in r-direction

$$\epsilon_{rr} = \frac{\partial u_r}{\partial r} \quad (4)$$

Normal Strain in θ direction

$$\epsilon_{\theta\theta} = \frac{1}{r} \left(\frac{\partial u_\theta}{\partial \theta} + u_r \right) \quad (5)$$

Normal Strain in the z-direction

$$\epsilon_{zz} = \frac{\partial u_z}{\partial z} \quad (6)$$

Shear Strain on r-plane

$$\gamma_{r\theta} = \frac{1}{2} \left(\frac{1}{r} \frac{\partial u_r}{\partial \theta} + \frac{\partial u_\theta}{\partial r} - \frac{u_\theta}{r} \right) \quad (7)$$

Shear Strain on θ plane

$$\gamma_{\theta z} = \frac{1}{2} \left(\frac{1}{r} \frac{\partial u_z}{\partial \theta} + \frac{\partial u_\theta}{\partial z} \right) \quad (8)$$

Shear Strain on z-plane

$$\gamma_{zr} = \frac{1}{2} \left(\frac{\partial u_r}{\partial z} + \frac{\partial u_z}{\partial r} \right) \quad (9)$$

Normal Stress in r-direction

$$\sigma_r = \left[\frac{1 - \nu_{23}\nu_{32}}{E_2 E_3 \Delta} \right] \epsilon_{rr} + \left[\frac{\nu_{21} + \nu_{23}\nu_{31}}{E_2 E_3 \Delta} \right] \epsilon_{\theta\theta} + \left[\frac{\nu_{31} + \nu_{21}\nu_{32}}{E_2 E_3 \Delta} \right] \epsilon_{zz} \quad (10)$$

Normal Stress in θ direction

$$\sigma_\theta = \left[\frac{\nu_{21} + \nu_{23}\nu_{31}}{E_2 E_3 \Delta} \right] \epsilon_{rr} + \left[\frac{1 - \nu_{13}\nu_{31}}{E_1 E_3 \Delta} \right] \epsilon_{\theta\theta} + \left[\frac{\nu_{32} + \nu_{12}\nu_{31}}{E_1 E_3 \Delta} \right] \epsilon_{zz} \quad (11)$$

Normal Stress in the z-direction

$$\sigma_z = \left[\frac{\nu_{31} + \nu_{21}\nu_{32}}{E_2 E_3 \Delta} \right] \epsilon_{rr} + \left[\frac{\nu_{32} + \nu_{12}\nu_{31}}{E_1 E_3 \Delta} \right] \epsilon_{\theta\theta} + \left[\frac{1 - \nu_{12}\nu_{21}}{E_1 E_2 \Delta} \right] \epsilon_{zz} \quad (12)$$

Where,

$$\Delta = \frac{(1 - \nu_{12}\nu_{21} - \nu_{23}\nu_{32} - \nu_{13}\nu_{31} - 2\nu_{21}\nu_{32}\nu_{13})}{E_1 E_2 E_3}$$

Shear Stress on r-plane

$$\tau_{r\theta} = [G_{12}] \gamma_{r\theta} \quad (13)$$

Shear Stress in θ direction

$$\tau_{\theta z} = [G_{23}] \gamma_{\theta z} \quad (14)$$

Shear Stress in the z-direction

$$\tau_{zr} = [G_{31}] \gamma_{zr} \quad (15)$$

The primary governing equations are involved in the FEA analysis, which is mentioned in equations (1) to (15). These complicated equations are needed to be transformed to so call weak form using Galerkin's method and thereby the element formulations are constructed. For static analysis this equation is:

$$[K]\{u\} = \{F\} \quad (16)$$

In general, static conditions are very low to represent the real-time problems thus the dynamic conditions more preferable to solve all kinds of structural problems. The equation (17) provides a dynamic analysis formulation:

$$[M]\{\ddot{u}\} + [C]\{\dot{u}\} + [K]\{u\} = \{F\} \quad (17)$$

Where [M] is the mass matrix, $[\ddot{U}]$ is the 2nd time derivative of the displacement [U] (i.e., the acceleration), $[\dot{U}]$ is the velocity, [C] is a damping matrix, [K] is the stiffness matrix, and [F] is the force vector. The computation tool first computes the displacements and then strain and from strains, it calculates stresses using a constitutive equation [11 - 22].

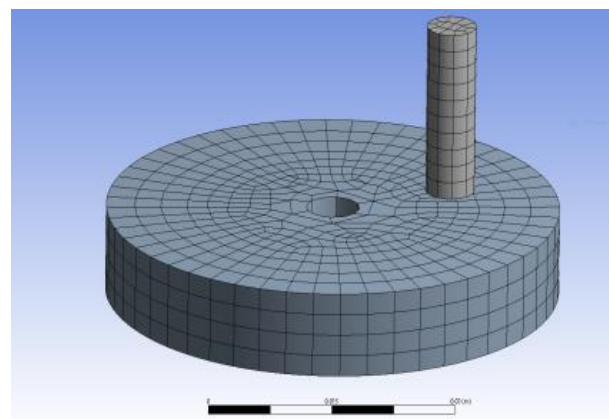
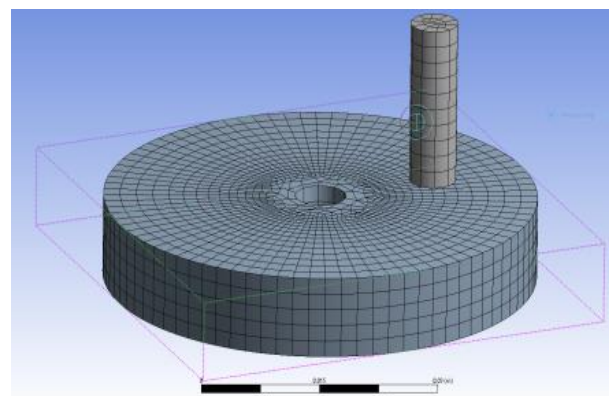
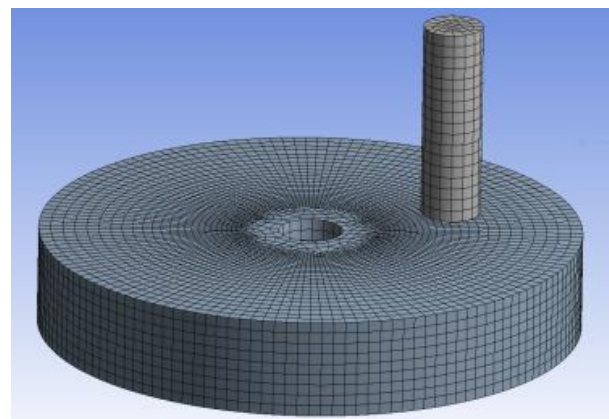
3.4 Grid Convergence Study of FEA

In simple, the grid convergence study is the optimization process of mesh, which is based

on its good quality with respect to providing the better outcome. The principle of this grid investigation is the estimation of output variations on all the mesh cases and thereby selects the least quantity of elements based on the tiny variations between the cases, in which the quality never treated as compromised one. In this grid optimization, a total of six different types of meshes are generated based on its capturing quality, which are coarse mesh, medium mesh, fine mesh, fine with proximity, fine with individual face set-up, and fine with inflation. The aforesaid boundary conditions are implemented in all the five cases, in which the Kevlar composite is commonly used for all the cases without a change in any kind of modifications. The first case deals with the coarse mesh set-up, which is revealed in Fig. 1. Medium quality based elements are constructed in the case - II, which is revealed in Fig. 2. Apart from these two cases, the advanced four more mesh cases are used in this work, which is fine with curvature set-up, fine with face mesh set-up, fine with curvature cum proximity set-up, and fine with inflation set-up. The advanced fine meshes are pictorially revealed in Figs. 3-5. The curvature and proximity facilities are more capable to capture warp and area variations regions henceforth those facilities are applied in the case - IV meshes. The top surface of the disc and bottom surface of the pin is important regions in the stress induction, thus the face mesh facilities are implemented in those regions in the case - V. Finally, inflation plays a major role in the construction of case - VI, in which the growth rate is fixed as 1.2. Generally, inflations are implemented in the primary region only, which is used in this work at the top surface of the disc. The comprehensive details of nodes and elements of all the mesh cases are listed in Table 2. And the computational structural analyses are computed for all the six different mesh-based Kevlar composite assigned test set-up, in which except the mesh variations all other input conditions are the same. The comparative data listed in Fig. 6, which concluded that case - IV is more preferable to use than other cases, thus case - IV based mesh set-ups are used for all the cases [23].

Table 2. Comparative Data of Mesh details.

Sl No	Type	Mesh Details	No of Nodes	No of Elements
1	Mesh - I	Coarse	8505	1692
2	Mesh - II	Medium	30973	6580
3	Mesh - III	Fine	84126	12954
4	Mesh - IV	Fine with Proximity	102584	20857
5	Mesh - V	Fine with face mesh set-up	150004	34103
6	Mesh - VI	Fine with inflation	161138	81381

**Fig. 1.** Coarse Mesh.**Fig. 2.** Medium Mesh.**Fig. 3.** Fine Mesh.

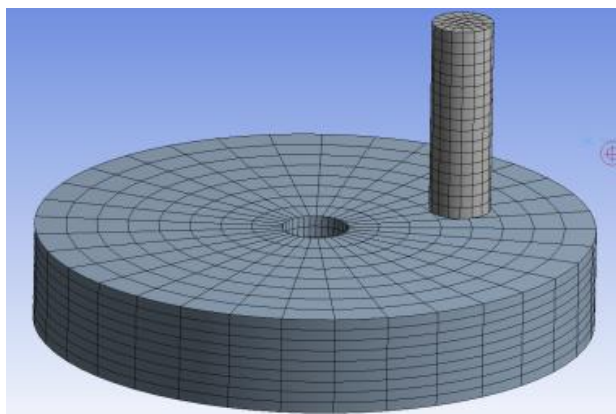


Fig. 4. Fine with face Mesh Set-Up.

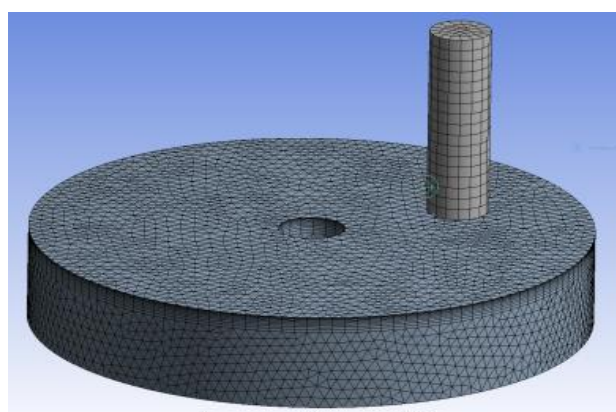


Fig. 5. Fine Mesh with Inflation set-Up.

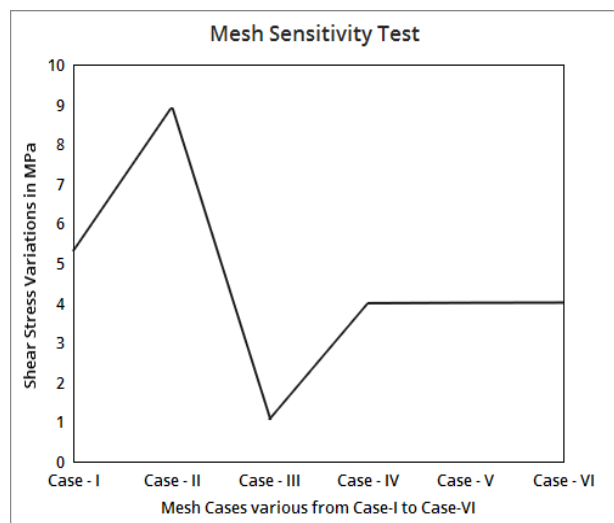


Fig. 6. Comprehensive data of Kevlar based composites.

3.5 Specimen Preparation using Compression molding

In this work, experimental tests are used to increase the reliability of the FEA results with the help of validation. Compression molding is a high-volume, high-pressure method suitable for molding complex, also used to prevent the voids of the composite laminates. Compression molding is the process of hot to produce semi-finished

parts. It takes the powdered particles of the material and produces a product under heat and pressure. Fabricated composite laminates are placed in the compression molding for curing. Voids are introduced during the manufacturing of composite laminates [24]. The top plate of the compression molding is set to a pressure of 100 kPa at 150 °C for 24 hours for released the voids from the laminates. The void contents are estimated from the test specimen, in which the value is obtained as 0.8 %. The preparation process of laminates and its predominant elements are revealed in the Figs. 7 and 8. In which carbon-woven-preperg-230GPa based fiber used as reinforcement and LY556 Epoxy resin cum XY 951 - Hardener are mixed and used as a matrix, finally, SiC is used as filler. The common name of this material used in this work is Carbon Ceramic Matrix Composite (CCMC).



Fig. 7. Carbon Fiber.



Fig. 8. Epoxy with hardener.

3.6 Procedure for Pin on Disc Wear Testing

Wear is related to interactions between surfaces and specifically the removal and deformation of material on a surface as a result of mechanical action of the opposite surface. The pin-on-disc configuration is commonly used to wear tests in laboratories because of its simple arrangement. Pin on disc tribometer is used to find the wear characteristics of the specimen. A pin on disc tribometer consists of a stationary "pin" under an applied load in contact with a rotating disc. The pin can have any shape to simulate a specific contact, but spherical tips are often used to simplify the contact geometry. The coefficient of friction is determined by the ratio of the frictional force to the loading force on the pin. Wear rate can be calculated by measuring the weight of the specimen before and after testing. In pin on disc tribometer, the material wear rate is a function of load applied, sliding speed, and the sliding distance. Wear track is formed on the specimen having the width equal to the diameter of the pin. The hardness of the pin should be larger than the specimen [25].

4. RESULTS AND DISCUSSION

4.1 FEA Results – Epoxy-Carbon-SiC composites

As stated earlier, four major CFRP based CMCs are underwent FEA analysis and thus obtained as the Epoxy-Carbon-Woven-Prepreg-SiC based composite is better than other CFRP-SiC composites. The Carbon-SiC based composite laminates of the FEA model as per the ASTM standard are developed using the Layered brick element. The Carbon-SiC based composite laminates are modeled using 3-D structural and finer mesh is used for the FEA model. From FEA results, it is observed that the maximum deformation occurred is 0.037257 mm, Maximum shear stress 0.025157 MPa and Maximum equivalent stress induced is 0.30603 MPa for Carbon-SiC based composite test specimen and the sample FEA results are shown in Figs. 9-11. In the specimens, maximum shear stress occurred at the edge of the specimen and maximum shear stress is 0.025157 MPa as shown in Fig. 10. The results of deformation, equivalent stresses, and shear stresses for various Carbon Ceramic Matrix Composite cases clearly explained that maximum deflection occurred at the edge of the brake disc

and the maximum resisting forces created at the fixed end, which are fulfilled and comes under the basic strength of materials theory. The numerical simulation of Carbon-SiC based composite laminates values of stresses and maximum deformation are fully revealed in Figs. 15-17. The FEA simulation results are within permissible limit and also suggested the application of Carbon-SiC based composite test specimen as a strengthening material to be useful for aircraft brake disc components. From the FEA study and thus von-mises stress distributions, the initial failure occurred in the edge of the brake disc, when equivalent stress reached to the ultimate level in the Epoxy Carbon Woven Prepreg SiC composite specimen compared to other Carbon fiber based SiC composites.

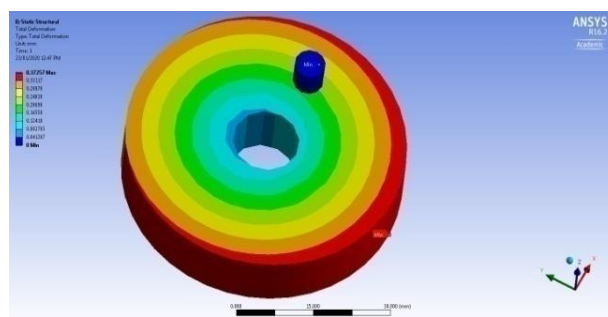


Fig. 9. Deformed variations on Epoxy Carbon Woven - Prepreg – SiC-based test specimen.

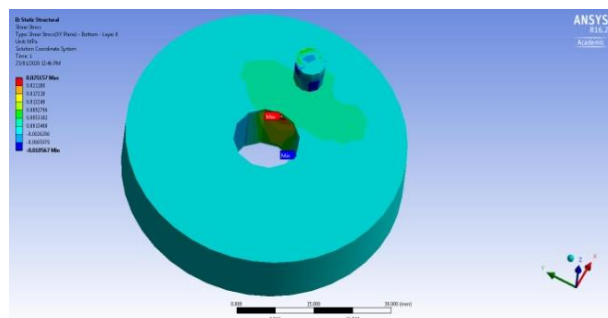


Fig. 10. Analysis result of Shear stress variations for Epoxy Carbon Woven - Prepreg – SiC.

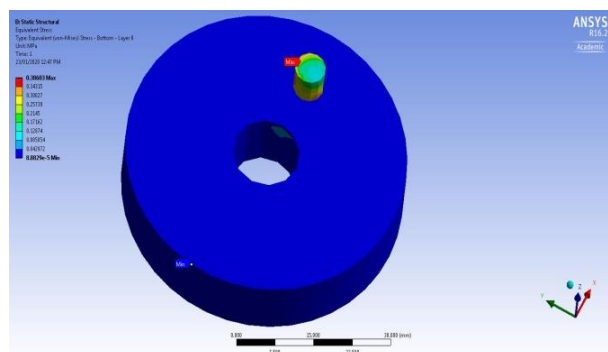


Fig. 11. Analysis result of equivalent stress variations for Epoxy Carbon Woven - Prepreg – SiC.

4.2 FEA Results – Epoxy-Glass-SiC composites

As stated earlier, three major GFRP based CMCs are underwent FEA analysis and thus obtained as the Epoxy E-Glass Uni-Directional (UD)-SiC based composite is better than other GFRP-SiC composites. The FEA models of all the test specimens are developed as per ASTM standard and constructed using ANSYS ACP 16.2, which is a unique tool for the composite construction. The Epoxy E-Glass-UD-SiC based composite laminates are modeled using 3-D structural elements and finer mesh is used for the FEA model. From FEA results, it is observed that the maximum deformation occurred is 0.040358 mm, Maximum shear stress 0.042825 MPa and Maximum equivalent stress induced is 0.3722 MPa for Glass-SiC based composite test specimen as shown in Figs. 12-14. In the specimens, maximum shear stress occurred at the center of the specimen and maximum shear stress is 0.042825 MPa as shown in Fig. 14. The results of deformation, equivalent stresses, and shear stresses for various cases clearly explained that maximum deflection occurred at the center of the brake disc specimen and the maximum resisting forces created at the fixed end, which are fulfilled the basic strength of materials' theory [1-8]. From the FEA study and von mises stress distributions, the initial failure occurred in the edge of the rotating disc, when equivalent stress reached to the ultimate level in the Epoxy E-Glass-UD-SiC composite specimen compared to the other Glass fiber based SiC composites.

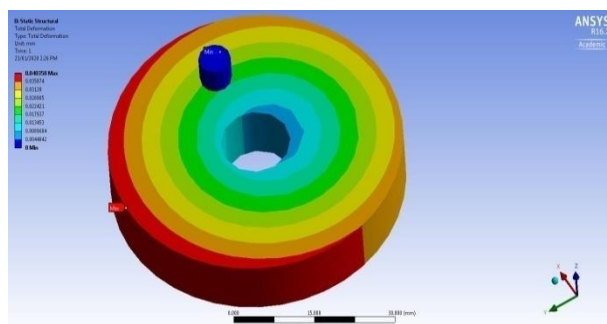


Fig. 12. Analysis result of the deformed test specimen for Epoxy E-Glass UD - Prepreg – SiC.

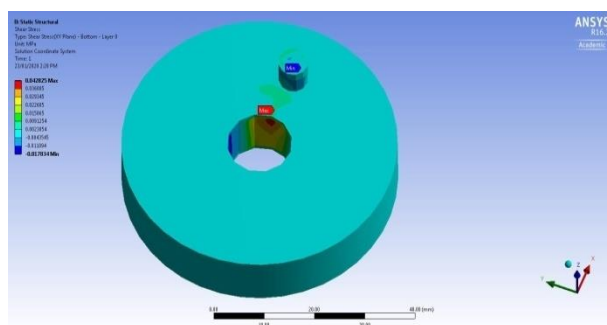


Fig. 13. Analysis result of Shear stress variations for Epoxy E-Glass UD - Prepreg – SiC.

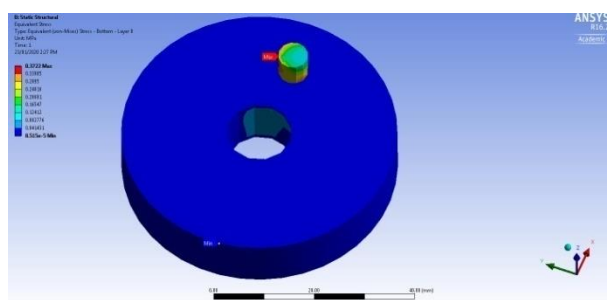


Fig. 14. Analysis result of Equivalent stress variations for Epoxy E-Glass UD - Prepreg – SiC.

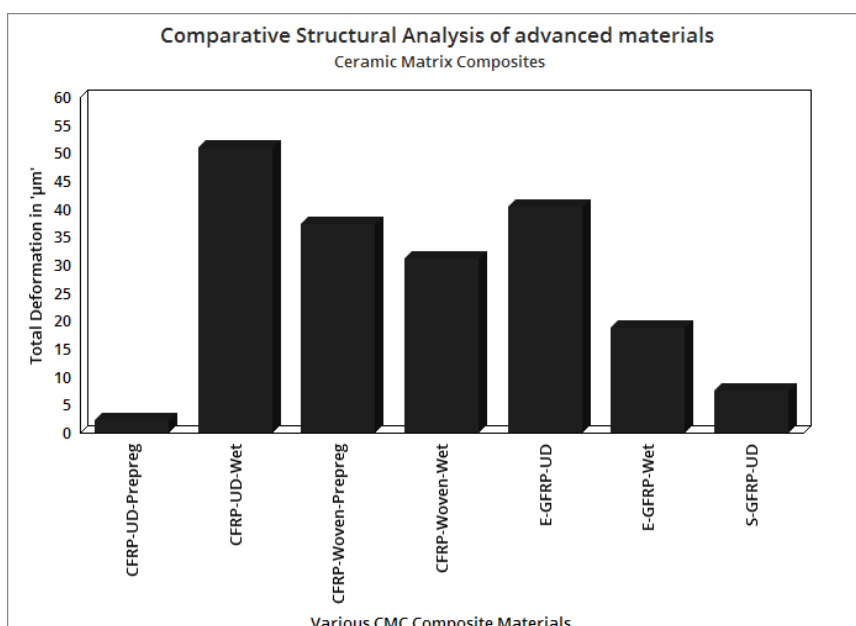


Fig. 15. Comparative deformation analysis of advanced materials.

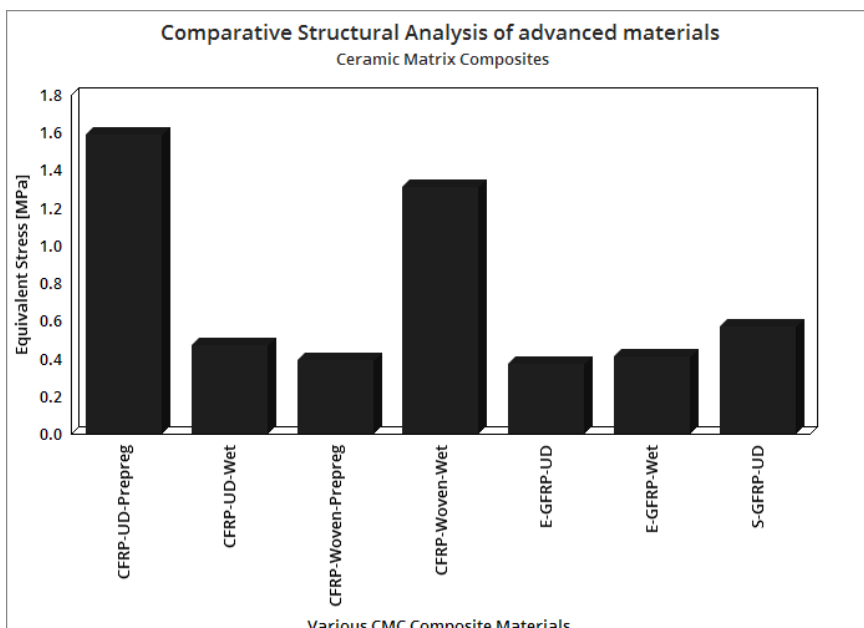


Fig. 16. Comparative Equivalent stress Analysis of advanced materials.

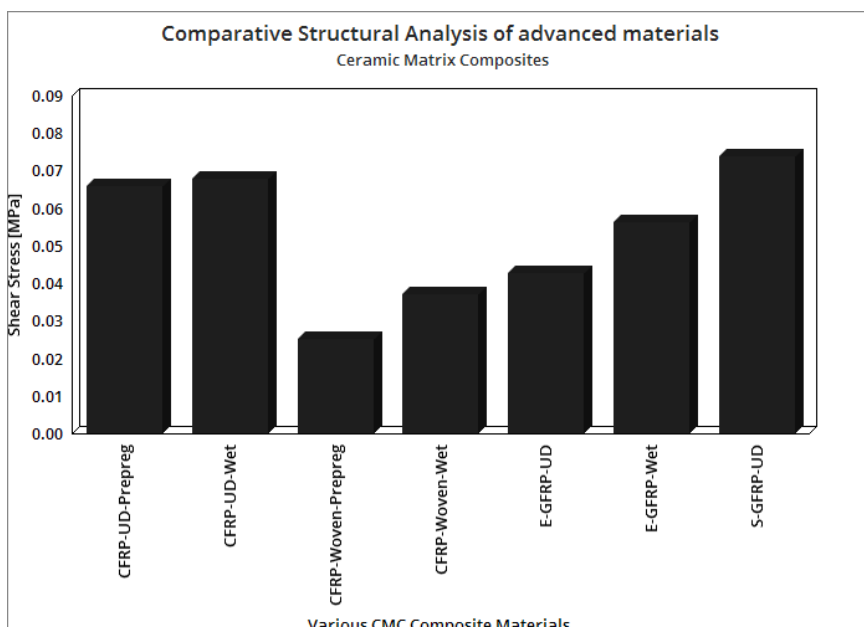


Fig. 17. Comparative shear stress analysis of advanced materials.

4.3 FEA Results for Conventional Composites

With the help of aforesaid boundary conditions and optimized grids through grid convergence study, the base composite materials are analyzed for comparison with advanced composite's outcomes. In these analyses, the primary elements such as various reinforcements and common Epoxy resins are used and thus four different cases are formed. The comprehensive structural outcomes are revealed in Figs. 18-20, in which primarily Kevlar, GFRP and CFRP based composites are used.

From the Figs. 15-17, it is obtained that CFRP Woven Prepreg fiber based SiC composite is better than all other composites, in which the selection is based on low induced level of shear stress therefore the same composite material is short-listed as the best option for the rotating disc-based real-time application. Also to get depth idea about the shear stress induction at the advanced composites, the comparison must be executed in between advanced composites and based composites. From the second cum base comparative analysis (Figs. 18-20), it is understood that Epoxy-Carbon-UD-230GPa-Prepreg is reacted

low shear stress than other base composites. Finally, SiC-based composites are performed well than without SiC composites in the shear stress perspective. Especially all the glass fiber composites are performed well with SiC than

carbon fiber composites. But based on the low reacted scale, the Epoxy Carbon Woven-Prepreg-SiC is chosen. Furthermore, the experimental based validation is completed to increase the reliability of the FEA results.

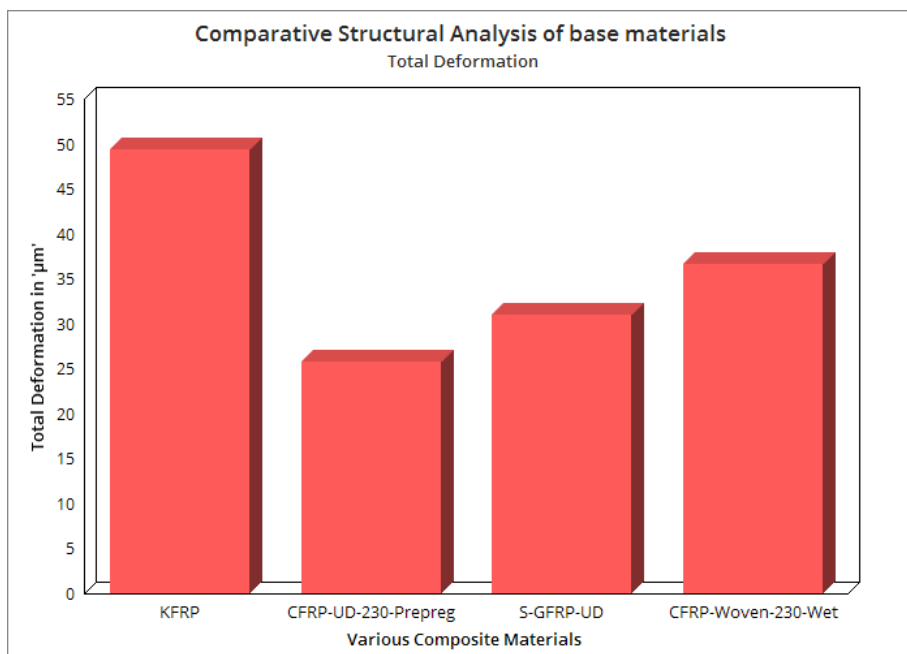


Fig. 18. Comparative Structural Analysis of base materials.

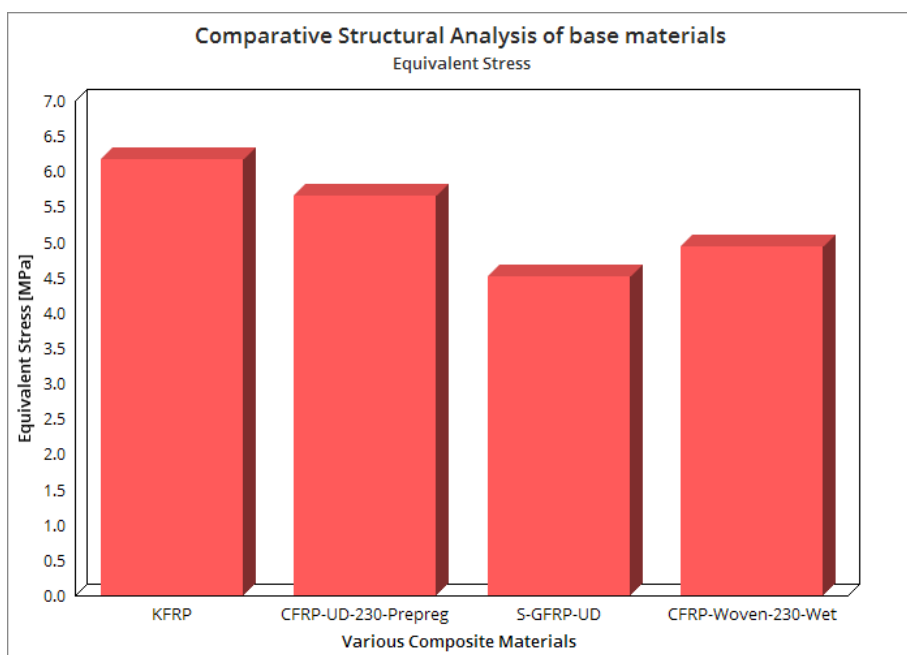


Fig. 19. Comparative Structural Analysis of base materials.

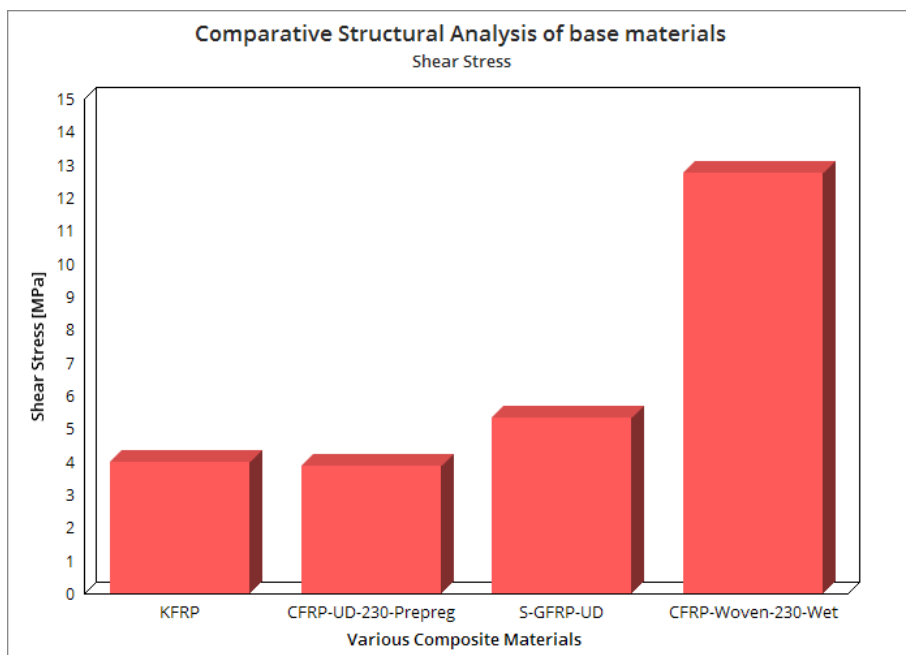


Fig. 20. Comparative Structural Analysis of base materials.

4.4 Experimental Results

The pin on the disc experiment is conducted for the given rotational velocity of 600 RPM. In which the environmental conditions are maintained correctly to decrease the environmental cum human error.



Fig. 21. Pin on Disc Wear Testing Experiment Setup.



Fig. 22. Wear vs Time-600 RPM for Epoxy Carbon - Prepreg - SiC.

The test specimen and instruments are shown in Fig. 21. The tests are conducted CCMC based composites, in which the ASTM G-99 provided all the relevant data. Figure 22 is revealed the pin on the disc output chart of Epoxy-Carbon-Woven-Prepreg-SiC.

This work confirms the applicability of Epoxy-Carbon-woven-Prepreg-SiC specimen as a good reinforcing agent, and also suggested the application of CFRP as a strengthening material to be used in the fabrication of rotating components. From the results, Epoxy-Carbon-woven-Prepreg-SiC's specimen withstands better wear resistance and good temperature capability than the other materials.

4.5 Validation Investigations

Table 3 provided the displacement-based comparative analyses in between two different approaches.

Table 3. Comparative study of results- 600 RPM.

Materials	Epoxy Carbon Woven - Prepreg - SiC	CCMC
	Numerical Simulation Results	Experimental Results
Deformation (mm)	0.037257	0.036027519
Wear rate (microns)	12	12
Frictional force (N)	4	4
Co-efficient of Friction	0.15	0.15

Thus the error percentage has been calculated and thus the value is obtained as 3.3 %. Because of this low error, the FEA results are validated and thus the proposed advanced composite materials are accepted for real-time applications. The experimental results of tribological outcomes listed in the Table 3 are included in the FEA analysis, which decreased the displacement's difference of both the approaches.

5. CONCLUSION

The objective of this study is to optimize the best material based on the investigation of the mechanical cum tribological behavior of various fiber-reinforced composites of rotating applications using experimental and FEA study. From FEA results, it is observed that the Epoxy-Carbon-Woven-Prepreg-SiC based composite test specimen is better than other composites because of its low reacting capability under rotodynamic loading. Also, understood that the outcomes induced in Carbon-Woven-Prepreg-SiC is fifty times lesser than other base composite materials. In which, the reacted structural cum tribological outcomes are total deformation as 0.037257 mm, shear stress as 0.025157 MPa and equivalent stress as 0.30603 MPa also the same deformation result is compared with pin on disc experimental results of CCMC (0.036027519). The error percentage is obtained as 3.3 % because of the implementation of perfect boundary conditions and sensitivity tests. Also, the through experimental test, the wear rate of the CMC is tested and obtained as 12 microns and coefficient of friction evaluated as 0.15. With these outcomes, this work concluded that applicability of Epoxy-Carbon-Woven-Prepreg-SiC composite material is the best material to withstand highly under rotodynamic loads and also suggested that Epoxy-E-Glass-UD-SiC capable for the aforesaid loading withstands. Carbon-Woven-Prepreg-SiC and Epoxy-E-Glass-UD-SiC are the best strengthening materials to be used for fabrication of rotating component such as aircraft and automotive disc brakes.

REFERENCES

[1] A. Daoud, M.T. AbouEl-Khair, *Wear and friction behavior of the Sand-cast brake rotor made of*

A359-20vol%SiC particle composites sliding against automobile friction material, Tribology International, vol. 43, iss. 3, pp. 544-553, 2010, doi: [10.1016/j.triboint.2009.09.003](https://doi.org/10.1016/j.triboint.2009.09.003)

- [2] A. Patnaik, A. Satapathy, S.S. Mahapatra, R.R. Dash, *A Comparative Study on Different Ceramic Fillers Affecting Mechanical Properties of Glass-Polyester Composites*, Journal of Reinforced Plastics and Composites, vol. 28, iss. 11, pp. 1305-1318, 2009, doi: [10.1177/0731684407086589](https://doi.org/10.1177/0731684407086589)
- [3] M. Alsaadi, A.A. Uгла, A. Erklig, *A comparative study on the inter-laminar shear strength of carbon, glass, and Kevlar fabric/epoxy laminates filled with SiC particles*, Journal of Composite Materials, vol. 51, iss. 20, pp. 2835-2844, 2017, doi: [10.1177/0021998317701559](https://doi.org/10.1177/0021998317701559)
- [4] Q.F. Guan, G.Y. Li, H.Y. Wang, J. An, *Friction-wear characteristics of carbon fiber reinforced friction material*, Journal of Materials Science, vol. 39, pp. 641-643, 2004, doi: [10.1023/B:JMSE.0000011520.48580.fc](https://doi.org/10.1023/B:JMSE.0000011520.48580.fc)
- [5] L.M. Manocha, G. Prasad, S. Manocha, *Carbon-Ceramic Composites for Friction Applications*, Mechanics of Advanced Materials and Structures, vol. 21, iss. 3, pp. 172-180, 2014, doi: [10.1080/15376494.2013.834095](https://doi.org/10.1080/15376494.2013.834095)
- [6] W. Li, X. Yang, S. Wang, J. Xiao, Q. Hou, *Comprehensive Analysis on the Performance and Material of Automobile Brake Discs*, Metals, vol. 10, iss. 3, p. 377, 2020, doi: [10.3390/met10030377](https://doi.org/10.3390/met10030377)
- [7] F.M. Mohammed, D.A. Smaït, *Mechanical and Tribological Behavior of Glass-Polyester Composite System Under Graphite Filler Content*, Engineering & Technology Journal, vol. 30, iss. 4, pp. 672 - 683, 2012.
- [8] G. Cueva, A. Sinatora, W.L. Guessier, A.P. Tschiptschin, *Wear resistance of cast irons used in brake disc rotors*, Wear, vol. 255, iss. 7-12, pp. 1256-1260, 2003, doi: [10.1016/S0043-1648\(03\)00146-7](https://doi.org/10.1016/S0043-1648(03)00146-7)
- [9] J.D. James D, S. Manoharan, G. Saikrishnan, S. Arjun, *Influence of Bagasse /Sisal Fibre Stacking Sequence on the Mechanical Characteristics of Hybrid-Epoxy Composites*, Journal of Natural Fibers, vol. 17, iss. 10, pp. 1497-1507, 2020, doi: [10.1080/15440478.2019.1581119](https://doi.org/10.1080/15440478.2019.1581119)
- [10] G. Suresh, L.S. Jayakumari, K.S. Dinesh, *Finite Element Analysis of IPN Reinforced Woven Fabric Composite*, Matéria (Rio de Janeiro), vol. 22, no. 4, p. 6, 2017, doi: [10.1590/s1517-707620170004.0216](https://doi.org/10.1590/s1517-707620170004.0216)
- [11] J. Kukutschova, V. Roubicek, K. Malachova, Z. Pavlickova, R. Holusa, J. Kubackova, V. Micka, D.

- MacCrimmon, P. Filip, *Wear mechanism in automotive brake materials, wear debris and its potential environmental impact*, *Wear*, vol. 267, iss. 5-8, pp. 807-817, 2009, doi: [10.1016/j.wear.2009.01.034](https://doi.org/10.1016/j.wear.2009.01.034)
- [12] F.-h. Su, Z.-z. Zhang, W.-m. Liu, *Mechanical and tribological property of Carbon Fabric composites filled with several nano particulates*, *Wear*, vol. 260, iss. 7-8, pp. 861-868, 2006, doi: [10.1016/j.wear.2005.04.015](https://doi.org/10.1016/j.wear.2005.04.015)
- [13] T.O. Larsen, T.L. Andersen, B. Thorning, A. Horsewell, M.E. Vigild, *Comparison of friction and wear for an epoxy reinforced by a glass or carbon/aramid hybrid weave*, *Wear*, vol. 262, iss. 7-8, pp. 1013-1020, 2007, doi: [10.1016/j.wear.2006.10.004](https://doi.org/10.1016/j.wear.2006.10.004)
- [14] B. Suresha, G. Chandramohan, P. Sampathkumaran, S. Sethuramu, *Investigation of the friction and wear behavior of glass-epoxy composite with and without graphite filler*, *Journal of Reinforced Plastics and Composites*, vol. 26, iss. 1, pp. 81-93, 2007, doi: [10.1177/0731684407069958](https://doi.org/10.1177/0731684407069958)
- [15] A.G. Adeniyi, S.A. Adeoye, D.V. Onifade, J.O. Ighalo, *Multi-scale finite element analysis of effective elastic property of sisal fiber-reinforced polystyrene composites*, *Mechanics of Advanced Materials and Structures*, 2019, doi: [10.1080/15376494.2019.1660016](https://doi.org/10.1080/15376494.2019.1660016)
- [16] G. Suresh, S.S. Bernard, S. Vivek, G.S. Krishnan, V.A. Kishore, A.I. Paul, K.M. Fowzan, *Study of mechanical performance of E-Glass fiber reinforced (IPN) interpenetrating polymer networks*, *Materials Today: Proceedings*, In Press, 2020, doi: [10.1016/j.matpr.2020.02.332](https://doi.org/10.1016/j.matpr.2020.02.332)
- [17] S.A. Bello, J.O. Agunsoye, J.A. Adebisi, N.K. Raji, S.B. Hassan, *Wear resistance properties of epoxy aluminium microparticle composite*, *Proceedings on Engineering Sciences*, vol. 1, no.1, pp. 58-65, 2019, doi: [10.24874/PES01.01.007](https://doi.org/10.24874/PES01.01.007)
- [18] A.G. Adeniyi, A.S. Adeoye, J.O. Ighalo, D.V. Onifade, *FEA of effective elastic properties of banana fiber-reinforced polystyrene composite*, *Mechanics of Advanced Materials and Structures*, 2020, doi: [10.1080/15376494.2020.1712628](https://doi.org/10.1080/15376494.2020.1712628)
- [19] M. Bak K, K. Kalaichelvan, *Experimental Study on the Mechanical Characterization of Glass-Basalt Fiber Reinforced Polymer (FRP) Composites*, *International Journal of Materials Science and Engineering*, vol. 4, no. 1, pp. 46-53, 2016, doi: [10.17706/ijmse.2016.4.1.46-53](https://doi.org/10.17706/ijmse.2016.4.1.46-53)
- [20] G. Suresh, L.S. Jayakumari, *Evaluating the mechanical properties of E-Glass fiber/carbon fiber reinforced interpenetrating polymer networks*, *Polímeros*, vol. 25, no. 1, pp. 49-57, 2015, doi: [10.1590/0104-1428.1650](https://doi.org/10.1590/0104-1428.1650)
- [21] H. Yanar, G. Purcek, H.H. Ayar, *Effect of cashew nut shell liquid (CNSL) on tribological behavior of brake pad composite*, *Proceedings on Engineering Sciences*, vol. 1, no.1, pp. 341-346, 2019, doi: [10.24874/PES01.01.044](https://doi.org/10.24874/PES01.01.044)
- [22] K. Venkatesan, K. Ramanathan, R. Vijayanandh, S. Selvaraj, G.R. Kumar, M.S. Kumar, *Comparative structural analysis of advanced multi-layer composite materials*, *Materials Today: Proceedings*, vol. 27, iss. 3, pp. 2673-2687, 2020, doi: [10.1016/j.matpr.2019.11.247](https://doi.org/10.1016/j.matpr.2019.11.247)
- [23] G.R. Kumar, M.S. Kumar, R. Vijayanandh. K.R. Sekar, K.M. Bak, S. Varun, *The Mechanical Characterization Of Carbon Fiber Reinforced Epoxy with Carbon Nanotubes*, *International Journal of Mechanical and Production Engineering Research and Development*, vol. 9, iss. 1, pp. 243-255, 2019.
- [24] G.R. Kumar, R. Vijayanandh, M.S. Kumar, S.S. Kumar, *Experimental Testing and Numerical Simulation on Natural Composite for Aerospace Applications*, *ICC 2017, AIP Conference Proceedings*, vol. 1953, iss. 1, 2018, doi: [10.1063/1.5032892](https://doi.org/10.1063/1.5032892)
- [25] R. Vijayanandh, K. Venkatesan, M. Ramesh, G.R. Kumar, M.S. Kumar, *Optimization of Orientation Of Carbon Fiber Reinforced Polymer Based On Structural Analysis*, *International Journal of Scientific & Technology Research*, vol. 8, iss. 11, pp. 3020 – 3029, 2019.